Physics Letters B 810 (2020) 135802

Contents lists available at ScienceDirect

Physics Letters B

www.elsevier.com/locate/physletb

D meson mixing as an inverse problem

Hsiang-nan Li [a], Hiroyuki Umeeda [a,*], Fanrong Xu [b], Fu-Sheng Yu [c]

[a] Institute of Physics, Academia Sinica, Taipei, 115, Taiwan, Republic of China
[b] Department of Physics, Jinan University, Guangzhou 510632, People's Republic of China
[c] School of Nuclear Science and Technology, Lanzhou University, Lanzhou 730000, People's Republic of China

ARTICLE INFO

Article history:
Received 5 May 2020
Received in revised form 29 August 2020
Accepted 19 September 2020
Available online 22 September 2020
Editor: B. Grinstein

ABSTRACT

We calculate the parameters x and y for the D meson mixing in the Standard Model by considering a dispersion relation between them. The dispersion relation for a fictitious charm quark of arbitrary mass squared s is turned into an inverse problem, via which the mixing parameters at low s are solved with the perturbative inputs $x(s)$ and $y(s)$ from large s. It is shown that nontrivial solutions for x and y exist, whose values around the physical charm scale agree with the data in both CP-conserving and CP-violating cases. We then predict the observables $|q/p|-1\approx 2\times 10^{-4}$ and $Arg(q/p)\approx 6\times 10^{-3}$ degrees associated with the coefficient ratio for the D meson mixing, which can be confronted with more precise future measurements. Our work represents the first successful quantitative attempt to explain the D meson mixing parameters in the Standard Model.

How to understand the large D meson mixing in the Standard Model has been a long-standing challenge. Previous evaluations based on box diagrams [1–3], and on heavy quark effective field theory [4,5] led to the mixing parameters x and/or y far below the current data. The updated inclusive analysis [6], including next-to-leading-order QCD corrections, still gave small $x\sim y\simeq 6\times 10^{-7}$. Some authors [7–9] claimed that higher dimensional operators, for which the strong Glashow-Iliopoulos-Maiani (GIM) suppression [10] might be circumvented, yielded dominant contributions. This claim has not been verified quantitatively, which requires information on a large number of nonperturbative matrix elements. Another uncertainty in the heavy quark expansion originates from violation of the quark-hadron duality, which represents an error in the analytic continuation from deep Euclidean to Minkowskian domains. A simple phenomenological argument [11] indicated that 20% duality violation could explain the width difference in the presence of the GIM cancellation.

On the other hand, the exclusive approach, where the D meson mixing is extracted from hadronic processes, led to an enhancement by relevant long-distance effects [8,12–20]. Modern works along this direction, e.g., [18,20] showed that a half value of y was accounted for roughly with contributions from two-body decays, albeit the difficulty in taking account of other multi-body channels. Thus, the quantitative understanding is still not attained in this data-driven approach, while the order of magnitude of the mixing parameters was properly described.

The complexities are attributed to the notorious difficulty of charm physics: the charm scale is too heavy to apply the chiral perturbation theory and possibly too light to apply the heavy quark expansion. Moreover, the D meson mixing, strongly suppressed by the GIM mechanism, is sensitive to nonperturbative SU(3) breaking effects [21] characterized by the strange and down quark mass difference, and to CKM-suppressed diagrams with bottom quarks in the loop. On the contrary, the heavy quark expansion accommodates the data for the $B_{d,s}$ meson mixings satisfactorily [11,22].

In this letter we will analyze the D meson mixing in a novel approach based on a dispersion relation, which relates x and y for a fictitious D meson of an arbitrary mass. The dispersion relation is separated into a low mass piece and a high mass piece, with the former being treated as an unknown, and the latter being input from reliable perturbative results. We then turn the study of the D meson mixing into an inverse problem: the mixing parameters at low mass are solved as "source distributions", which produce the "potential" observed at high mass. It will be demonstrated that nontrivial correlated solutions for x and y exist, whose values around the physical charm quark mass $m_c\approx 1.3$ GeV match the data in both cases with and without CP violation. Our observation implies that resonance properties can be extracted from asymptotic QCD by solving an inverse problem.

Consider the analytical transition matrix element for a D meson formed by a fictitious charm quark of invariant mass squared s,

* Corresponding author.
E-mail address: umeeda@gate.sinica.edu.tw (H. Umeeda).

https://doi.org/10.1016/j.physletb.2020.135802

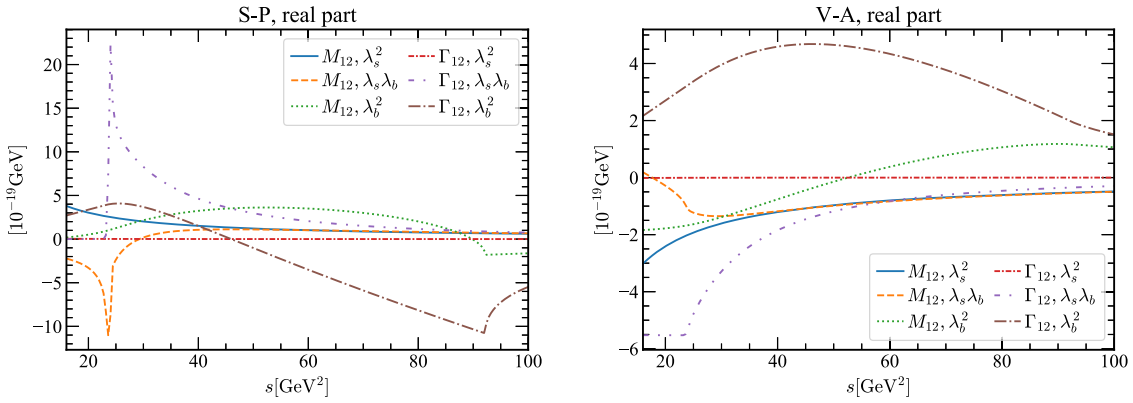

Fig. 1. λ_s^2, $\lambda_s\lambda_b$ and λ_b^2 contributions to the real parts of M_{12} and Γ_{12} from the $S-P$ and $V-A$ operators.

$$M_{12}(s) - \frac{i}{2}\Gamma_{12}(s) = \langle D^0(s)|\mathcal{H}_w^{\Delta C=2}|\bar{D}^0(s)\rangle, \tag{1}$$

whose branch cut runs from the threshold $s = 4m_\pi^2$ to infinity with the pion mass m_π. The effective weak Hamiltonian $\mathcal{H}_w^{\Delta C=2}$ contains two four-fermion operators $(V-A)(V-A)$ and $(S-P)(S-P)$, which will be abbreviated to $V-A$ and $S-P$ below, respectively. The right hand side of Eq. (1) starts with the evaluation of box diagrams, whose dispersive and absorptive contributions give rise to M_{12} and Γ_{12}, respectively. The dispersive part M_{12} and the absorptive part Γ_{12} then obey the dispersion relation [17]

$$M_{12}(s) = \frac{P}{2\pi}\int_0^\infty ds' \frac{\Gamma_{12}(s')}{s-s'}, \tag{2}$$

where P denotes the principal value prescription, and the lower bound of the integration variable s', being of $O(m_\pi^2)$, has been approximated by zero. Equation (1) governs the time evolution of the D^0 and $\bar{D}^0$ mesons, whose diagonalization yields the mass eigenstates $D_{1,2} = pD^0 \pm q\bar{D}^0$ as linear combinations of the weak eigenstates D^0 and $\bar{D}^0$. The mass and width differences of $D_{1,2}$ define the mixing parameters

$$x \equiv \frac{m_1 - m_2}{\Gamma} = \frac{2M_{12}}{\Gamma}, \quad y \equiv \frac{\Gamma_1 - \Gamma_2}{2\Gamma} = \frac{\Gamma_{12}}{\Gamma}, \tag{3}$$

in the CP-conserving case with the total decay width Γ. The elements M_{12} and Γ_{12}, extracted from the evaluation of box diagrams [1,2], can be applied to the mixing of a heavy meson with arbitrary mass, and will be adopted directly below. The b quark mass m_b should remain constant in the evaluation of Γ_{12}, so that the fictitious D meson can decay into a b quark, as its mass crosses the b quark threshold. The right hand side of Eq. (2) then contains heavy quark contributions to be consistent with the heavy quark dynamics involved in M_{12}. The $V-A$ contribution Γ_{12}^{V-A} is given, for $s > 4m_b^2$, by

$$\begin{aligned}\Gamma_{12}^{V-A} \propto{}& \lambda_s^2(B_{dd}^{(a)} - 2B_{ds}^{(a)} + B_{ss}^{(a)}) + 2\lambda_s\lambda_b(B_{dd}^{(a)} - B_{ds}^{(a)} - B_{db}^{(a)} \\ &+ B_{sb}^{(a)}) + \lambda_b^2(B_{dd}^{(a)} - 2B_{db}^{(a)} + B_{bb}^{(a)}),\end{aligned} \tag{4}$$

where $\lambda_k \equiv V_{ck}V_{uk}^*$, $k = s, b$, are the products of the Cabibbo-Kobayashi-Maskawa (CKM) matrix elements, and the functions $B_{ij}^{(a)}$ [2] with the internal quarks $i, j = d, s, b$ arise from the absorptive contributions of the box diagrams for Eq. (1). The terms up to $B_{ss}^{(a)}$ ($B_{db}^{(a)}$, $B_{sb}^{(a)}$) are kept in the range $s < (m_b + m_d)^2$ ($(m_b + m_d)^2 \le s < (m_b + m_s)^2$, $(m_b + m_s)^2 \le s < 4m_b^2$). The expression of the $S-P$ contribution Γ_{12}^{S-P} is similar but with $B_{ij}^{(a)}$ in Eq. (4) being replaced by $C_{ij}^{(a)}$ [2]. Equation (4) shows clearly that the D meson mixing results from the flavor symmetry breaking. We have confirmed that Γ_{12} deceases like $1/s^2$ at large s, so the integral on the right hand side of Eq. (2) converges.

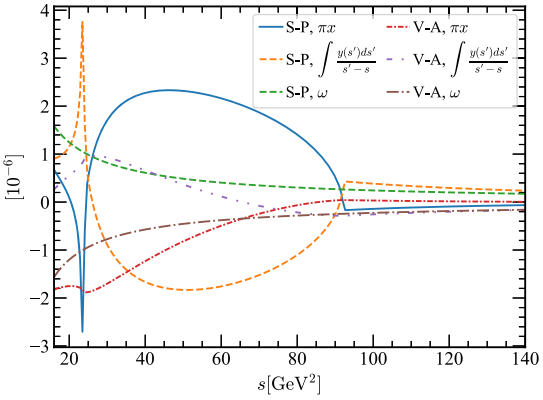

Fig. 2. Dispersive and absorptive contributions to the real part of $\omega(s)$ from the $S-P$ and $V-A$ operators.

We rewrite the dispersion relation as

$$\int_0^\Lambda ds' \frac{y(s')}{s-s'} = \pi x(s) - \int_\Lambda^\infty ds' \frac{y(s')}{s-s'} \equiv \omega(s), \tag{5}$$

where both sides have been divided by the measured total width $\Gamma_{\text{exp}} = 1.61 \times 10^{-12}$ GeV [23] to get the variables x and y. The separation scale Λ is arbitrary, but should be large enough to justify the perturbative calculation of y on the right hand side, and below the b quark threshold to avoid the b quark contribution to the left hand side. The product $f_D^2 m_D$ appearing in the expressions of M_{12} and Γ_{12} [2] on the right hand side of Eq. (5), with the D meson decay constant f_D and its mass m_D, scales like a constant in the heavy quark limit. Here we adopt the value for a B_s meson [23], i.e., $f_D^2 m_D \sim 0.3$ GeV^3. The behaviors of $M_{12}(s)$ and $\Gamma_{12}(s)$ from the $S-P$ and $V-A$ operators with the masses $m_d = 5$ MeV, $m_s = 109.9$ MeV, $m_b = 4.8$ GeV and $m_W = 80.379$ GeV, the separation scale $\Lambda = m_b^2/2 \approx 12$ GeV^2, and the bag parameters equal to unity are displayed in Fig. 1, which have been decomposed into three pieces proportional to the real parts of λ_s^2, $\lambda_s\lambda_b$ and λ_b^2. The above choice of Λ can be regarded as being of $O(m_b^2)$, so the perturbation theory is applicable to the mixing of the fictitious D meson for $s > \Lambda$. The choice of $m_s = 109.9$ MeV is within the range of the strange quark mass $m_s = 108^{+13}_{-6}$ MeV given for the renormalization scale $\mu = m_c$ in [23]. It is seen in Fig. 2 that both terms on the right-hand side of Eq. (5) exhibit cusps as s crosses the b quark and b quark pair thresholds. Their

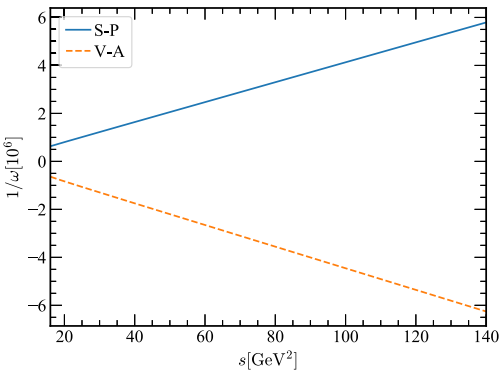

Fig. 3. s dependence of $1/\omega$.

sum $\omega(s)$ behaves smoothly and, furthermore, turns out to be independent of m_b. This feature, existent for the two four-fermion operators, indicates that y in the low mass region $s < \Lambda$ decouples from the b quark dynamics as expected.

In principle, we can have separate dispersion relations associated with the three CKM products. However, it is reasonable to combine all the terms in Eq. (4) into a single dispersion relation due to the dominance of the λ_s^2 contribution to the real part of $\omega(s)$. The $S-P$ and $V-A$ contributions are opposite in sign, and the corresponding bag parameters are roughly equal. The significant cancellation between these two pieces causes sensitivity to the bag parameters, which have not yet been computed precisely enough in lattice QCD. To reduce the sensitivity to this potential cancellation, we consider separate dispersion relations for these two operators. Equation (5) will be treated as an inverse problem, in which $\omega(s)$ for $s > \Lambda$ from Fig. 2 is an input, and $y(s)$ in the range $s < \Lambda$ is solved with the boundary condition $y(0) = 0$ and the continuity of y at $s = \Lambda$. That is, the "source distribution" $y(s)$ will be inferred from the "potential" $\omega(s)$ observed outside the distribution.

For such an ill-posed inverse problem, the ordinary discretization method to solve an integral (Fredholm) equation does not work. The discretized version of Eq. (5) is in the form $\sum_i A_{ij} y_j = \omega_i$ with $A_{ij} \propto 1/(i-j)$. It is easy to find that any two adjacent rows of the matrix A approach to each other as the grid becomes infinitely fine. Namely, A tends to be singular, and has no inverse. We stress that this singularity, implying no unique solution, should be appreciated actually. If A is not singular, the solution to Eq. (5) will be unique, which must be the tiny perturbative result obtained in the literature. It is the existence of multiple solutions that allows possibility to explain the observed large D meson mixing.

We notice that the smooth curves of $\omega(s)$ can be well described by simple functions proportional to $1/(s-m^2)$, as indicated by the almost straight lines for $1/\omega(s)$ down to $s = 15$ GeV^2 in Fig. 3. These straight lines, as extrapolating to the low s region, cross the horizontal axis at some small scale $s = m^2$. The power-law behavior is understandable, since only the effect from the monopole component of the distribution dominates at large s, which decreases like $1/s$. The meaning of the scale m^2 will become clear later. If $\omega(s)$ followed the power law exactly, the solution to Eq. (5) would be a δ-function, $y(s) \propto \delta(s-m^2)$. The slight deviation from the power-law behavior suggests mild broadening of $y(s)$ into a resonance-like distribution located at $s \approx m^2$, if $m^2 > 0$.

Viewing the difficulty to solve an inverse problem with multiple solutions and the qualitative resonance-like behavior of a solution, we propose the parametrization

$$y(s) = \frac{Ns[b_0 + b_1(s-m^2) + b_2(s-m^2)^2]}{[(s-m^2)^2 + d^2]^2}, \tag{6}$$

for $0 \le s \le \Lambda$, and determine the free parameters b_0, b_1, b_2, m^2 and d from the best fit to the input $\omega(s)$. The normalization N respects $Ns/[(s-m^2)^2+d^2]^2 \to \delta(s-m^2)$ in the vanishing width limit $d \to 0$. Equation (6) with the completely free parameters is general enough, which can also describe a nonresonant behavior with $m^2 < 0$ and a flat behavior with large d. The convergence of the expansion in the numerator will be verified, so keeping terms up to $(s-m^2)^2$ is sufficient. Equation (6) obeys the boundary condition $y(0) = 0$. The continuity of $y(s)$ at $s = \Lambda$, i.e., the equality of $y(\Lambda)$ to the perturbative input imposes a constraint among the five parameters. We emphasize that a systematic expansion of $y(s)$ in terms of a complete basis of orthogonal functions also works, but the numerical analysis is more tedious, and will be performed in a forthcoming paper.

The separation scale Λ introduces an end-point singularity to the integral on the right hand side of Eq. (5), as $s \to \Lambda$. To reduce the effect caused by this artificial singularity, we consider $\omega(s)$ from the range 30 GeV$^2 < s <$ 250 GeV^2, in which 200 points s_i are selected. We have checked the cases with 100, 200 and 300 points, and confirmed that the results have little dependence on these numbers. For each point (m^2, d) on the m^2-d plane, we search for b_0 and b_1, that minimize the deviation

$$\sum_{i=1}^{200} \left| \int_0^\Lambda ds' \frac{y(s')}{s_i - s'} - \omega(s_i) \right|^2 . \tag{7}$$

The above definition, characterizing the relative quality of solutions, is referred to as the goodness-of-fit (GOF) hereafter. The value of b_2 is fixed by the continuity constraint at $s = \Lambda$. The scanning on the m^2-d plane generates the arc-shaped distribution of the GOF minima associated with the $S-P$ operator in Fig. 4, which ranges roughly in -0.2 GeV$^2 < m^2 < 1.8$ GeV^2. The minima along the arc, having similar GOF about 10^{-21}-10^{-22} relative to 10^{-17} from outside the arc, hint the existence of multiple solutions. If a resonance-like solution with $m^2 \sim m_c^2$ and small d exists, i.e., obeys the dispersion relation, it will be revealed by the scanning, and indeed it is as shown in Fig. 4.

Evaluating $y(s)$ at low s in perturbation theory with a finite running coupling constant α_s, we get different results at various orders. These different results lead to almost identical $\omega(s)$ in the large s limit, where α_s diminishes. The solutions from m^2 away from m_c^2 might correspond to fixed-order results, since they generate tiny y at the physical scale m_c^2, while those near $m^2 \approx m_c^2$ correspond to nonperturbative results. We select a typical nonresonant solution for $y(s)$ with $m^2 = 0$ and $d = 0.38$ GeV^2 from the arc associated with the $S-P$ operator, and compare it to a resonance-like solution with $m^2 = 1.713$ GeV^2 and $d = 3.876 \times 10^{-2}$ GeV^2 from the same arc in Fig. 5. The dramatic distinction in the shape and in the order of magnitude between these two cases supports that Eq. (6) is general enough to exhibit very different behaviors. The observation that the above perturbative and nonperturbative solutions give the same $\omega(s)$ at large s realizes the concept of the global quark-hadron duality postulated in QCD sum rules [24]. The arc-shaped distribution from the $V-A$ operator is also displayed in Fig. 4, where a solution with $m^2 \approx m_c^2$ has a large d, so its contribution to y is negligible.

Selecting a point (m^2, d) on the arc, we get a solution of $y(s)$. Substituting the obtained $y(s)$, i.e., $\Gamma_{12}(s)$ in the whole range of s into Eq. (2), we calculate the corresponding $x(s)$. The values $x(m_c^2)$ and $y(m_c^2)$ are then compared with the data. It is seen in the left plot of Fig. 6 that the data $x = (0.50^{+0.13}_{-0.14})\%$ and $y = (0.62 \pm 0.07)\%$ in the CP-conserving case [25] can be accommodated simultaneously by the $S-P$ contribution with the parameters

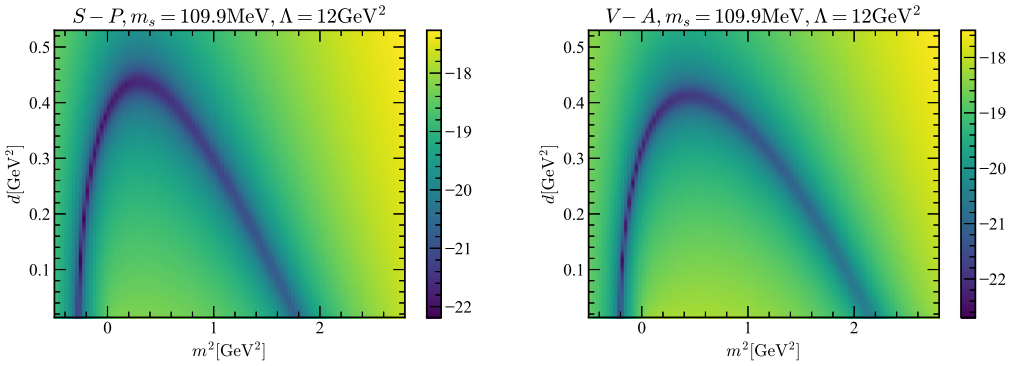

Fig. 4. Distributions of GOF minima in the common logarithmic scale on the m^2-d plane.

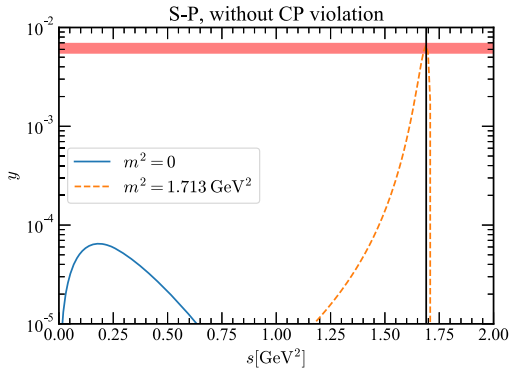

Fig. 5. Comparison of a typical nonresonant solution and a resonance-like solution for y. The horizontal band represents the data with 1σ errors, and the vertical line corresponds to $s = m_c^2$.

$$m^2 = 1.713\ \text{GeV}^2,\ \ d = 3.876 \times 10^{-2}\ \text{GeV}^2,$$
$$b_0 = -3.296 \times 10^{-5}\ \text{GeV}^2,\ \ b_1 = -3.234 \times 10^{-2},$$
$$b_2 = 5.617 \times 10^{-2}\ \text{GeV}^{-2}. \tag{8}$$

Equation (8) justifies that the lower bound of the integral in Eq. (2), being of $O(m_\pi^2)$, can be set to zero safely, because $y(s)$ takes substantial values only around $s \sim O(m_c^2)$. We remind that the values in Eq. (8) are representative, and their slight variations are allowed for explaining the data of x and y within 1σ. For instance, the width d is allowed to vary by 20%. The uncertainties from the fitting procedure and from the parametrization for $y(s)$ will be investigated rigorously in a subsequent publication.

It has been concluded [20] that two-body modes in D meson decays are insufficient for understanding y, and multi-particle modes play a crucial role for this purpose. When s increases, single strange quark channels with destructive contributions, like $KKK\pi$, are enhanced by phase space, and double strange quark channels with constructive contributions, like $KKKK$, are opened. This tendency fits the behavior of $y(s)$ in Fig. 6, which first decreases from a positive value expected in the two-body analysis [20] to a negative value, and then increases with s. It also explains why the width d, within which the above oscillation occurs, is of $O(m_s^2)$. As a single resonance around $s \approx m_c^2$ accommodates the data, it would hint that the multi-particle channels with the total rest mass around m_c give dominant contributions to y. Certainly, our observation does not exclude other shorter peaks at lower s but above the threshold for two-body channels. That is, the curve in Fig. 6 has caught the major features of $y(s)$, though its true behavior might be more complicated. We have also examined that the b_1 term dominates, and the b_2 term contributes only about 10% of $x(m_c^2)$ and $y(m_c^2)$. The convergence of the parametrization in Eq. (6) is verified. To test whether $x(m_c^2)$ and $y(m_c^2)$ exhibit a quadratic rise with m_s, as expected from the SU(3) symmetry breaking [8], we fix $\Lambda = 12\ \text{GeV}^2$ and $m^2 = 1.713\ \text{GeV}^2$ in Eq. (8), and then derive $x(m_c^2)$ and $y(m_c^2)$ from the dispersion relation for various m_s. The quadratic increase with a vanishing slope at small m_s is indeed observed.

As CP violation is allowed, both M_{12} and Γ_{12} become complex due to the weak phase in the CKM matrix elements, but Eq. (2) still holds. The expressions of x and y in terms of the complex M_{12} and Γ_{12} are referred to [23]. In this case the same parameters $\Lambda = 12\ \text{GeV}^2$ and $m_s = 109.9$ MeV are chosen, and the λ_b^2 contribution is found to dominate the imaginary part of $\omega(s)$. An additional parametrization similar to Eq. (6) but with primed parameters is proposed. The imaginary part of $\omega(s)$ is fitted by the primed parametrization independently of the fitting to its real part. The scanning on the m^2-d planes yields the arc-shaped distributions of the GOF minima similar to Fig. 4. Taking a common value for m^2 and m'^2, one finds that the real part of the $S-P$ contribution still dominates x and y. The parameters in Eq. (8) and

$$m'^2 = m^2 = 1.713\ \text{GeV}^2,\ \ d' = 4.970\ \text{GeV}^2,$$
$$b_0' = -8.238 \times 10^{-7}\ \text{GeV}^2,\ \ b_1' = 4.355 \times 10^{-7},$$
$$b_2' = -7.192 \times 10^{-8}\ \text{GeV}^{-2}, \tag{9}$$

for the $S-P$ imaginary contribution, and those for the $V-A$ contribution, which are not presented for simplicity, accommodate the data $x = (0.39^{+0.11}_{-0.12})\%$ and $y = (0.651^{+0.063}_{-0.069})\%$ [25] simultaneously, as illustrated in the right plot of Fig. 6. Given the parameters in Eqs. (8) and (9) and those of the $V-A$ contribution, we then derive $|q/p| - 1 \approx 2.2 \times 10^{-4}$ and $Arg(q/p) \approx (6.2 \times 10^{-3})^\circ$ associated with the coefficient ratio as predictions, which are comparable to the data $q/p = (0.969^{+0.050}_{-0.045})e^{i(-3.9^{+4.5}_{-4.6})^\circ}$ [25], and can be confronted with more precise measurements in future.

To examine the uncertainty from the theoretical input, we increase m_s to, say, 130.6 MeV, for which Λ needs to increase to 14 GeV^2 accordingly to accommodate the observed x and y. That is, a positive correlation between m_s and Λ is observed. In this case, the representative parameters for the real and imaginary parts of the $S-P$ contribution from the fit are

$$m^2 = m'^2 = 1.720\ \text{GeV},\ \ d = 5.467 \times 10^{-2}\ \text{GeV}^2,$$
$$d' = 5.267\ \text{GeV}^2,$$
$$b_0 = 7.989 \times 10^{-6}\ \text{GeV}^2,\ \ b_1 = -3.025 \times 10^{-2},$$
$$b_2 = 3.011 \times 10^{-2}\ \text{GeV}^{-2},$$
$$b_0' = -1.438 \times 10^{-6}\ \text{GeV}^2,\ \ b_1' = 6.680 \times 10^{-7},$$
$$b_2' = -8.870 \times 10^{-8}\ \text{GeV}^{-2}. \tag{10}$$

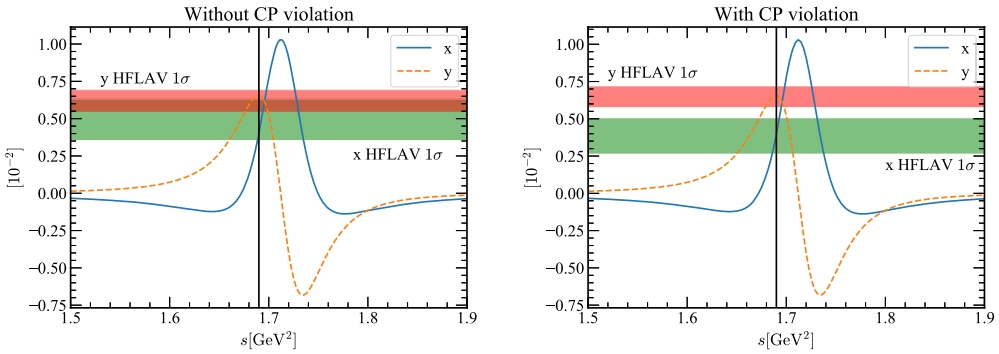

Fig. 6. $x(s)$ and $y(s)$ in the cases without and with CP violation.

Compared to Eqs. (8) and (9), the result of m^2 varies slightly, the dominant coefficient b_1 changes by 10% roughly, and d exhibits about 30% uncertainty. The above parameters, together with those for the $V-A$ contribution, lead to $|q/p|-1 \approx 3.2\times10^{-4}$ and $Arg(q/p) \approx (7.1\times10^{-3})^\circ$. It is seen that our predictions for $|q/p|-1$ and $Arg(q/p)$ are quite stable with respect to the variation of m_s, which change by only ∼10%-30%. That is, q/p can serve as an ideal observable for constraining new physics effects.

This work represents the first successful quantitative attempt in the sense that definite values have been presented for the D meson mixing parameters x and y in both the CP-conserving and CP-violating cases in the Standard Model. The key is to transform the dispersion relation between x and y into an inverse problem, in which the nonperturbative observables at low mass are solved with the perturbative inputs from high mass. It is nontrivial to find a solution under the analyticity constraint from the perturbative inputs that explains the data of x and y. The accommodation of the data by a single resonance around the charm mass hints that multi-particle channels of D meson decays give dominant contributions to y. If such a solution does not exist, it would be a strong indication that the large mixing parameters are attributed to new physics. The obtained solution has been employed to predict the coefficient ratio q/p in the CP-violating case. To improve the precision of our results, high-power corrections to the inputs can be included systematically. Theoretical uncertainties in this approach will be investigated in detail in the future. Once the D meson mixing is understood, relevant data, especially those for the coefficient ratio q/p, can be used to constrain new physics effects appearing in the box diagrams. Our approach will be developed into a fundamental nonperturbative QCD formalism, with the insight that resonance properties are extractable from asymptotic QCD as demonstrated in the D meson mixing case.

Declaration of competing interest

The authors declare that they have no known competing financial interests or personal relationships that could have appeared to influence the work reported in this paper.

Acknowledgement

This work was supported in part by MOST of R.O.C. under Grant No. MOST-107-2119-M-001-035-MY3, and by NSFC under Grant Nos. U1932104, 11605076, U173210, and 11975112.

References

[1] H.Y. Cheng, Phys. Rev. D 26 (1982) 143.
[2] A.J. Buras, W. Slominski, H. Steger, Nucl. Phys. B 245 (1984) 369.
[3] A. Datta, D. Kumbhakar, Z. Phys. C 27 (1985) 515.
[4] H. Georgi, Phys. Lett. B 297 (1992) 353–357.
[5] T. Ohl, G. Ricciardi, E.H. Simmons, Nucl. Phys. B 403 (1993) 605–632.
[6] E. Golowich, A.A. Petrov, Phys. Lett. B 625 (2005) 53.
[7] I.I. Bigi, N.G. Uraltsev, Nucl. Phys. B 592 (2001) 92–106.
[8] A.F. Falk, Y. Grossman, Z. Ligeti, A.A. Petrov, Phys. Rev. D 65 (2002) 054034.
[9] M. Bobrowski, A. Lenz, J. Riedl, J. Rohrwild, arXiv:0904.3971 [hep-ph], J. High Energy Phys. 1003 (2010) 009.
[10] S.L. Glashow, J. Iliopoulos, L. Maiani, Phys. Rev. D 2 (1970) 1285.
[11] T. Jubb, M. Kirk, A. Lenz, G. Tetlalmatzi-Xolocotzi, Nucl. Phys. B 915 (2017) 431–453.
[12] L. Wolfenstein, Phys. Lett. B 164 (1985) 170–172.
[13] J.F. Donoghue, E. Golowich, B.R. Holstein, J. Trampetic, Phys. Rev. D 33 (1986) 179.
[14] P. Colangelo, G. Nardulli, N. Paver, Phys. Lett. B 242 (1990) 71–76.
[15] F. Buccella, M. Lusignoli, G. Miele, A. Pugliese, P. Santorelli, Phys. Rev. D 51 (1995) 3478–3486.
[16] T.A. Kaeding, Phys. Lett. B 357 (1995) 151–155.
[17] A.F. Falk, Y. Grossman, Z. Ligeti, Y. Nir, A.A. Petrov, Phys. Rev. D 69 (2004) 114021.
[18] H.Y. Cheng, C.W. Chiang, Phys. Rev. D 81 (2010) 114020.
[19] M. Gronau, J.L. Rosner, Phys. Rev. D 86 (2012) 114029.
[20] H.Y. Jiang, F.S. Yu, Q. Qin, H.n. Li, C.D. Lü, Chin. Phys. C 42 (2018) 063101.
[21] R. Kingsley, S. Treiman, F. Wilczek, A. Zee, Phys. Rev. D 11 (1975) 1919.
[22] M. Artuso, G. Borissov, A. Lenz, Rev. Mod. Phys. 88 (2016) 045002.
[23] M. Tanabashi, et al., Particle Data Group, Phys. Rev. D 98 (2018) 030001.
[24] M.A. Shifman, arXiv:hep-ph/0009131.
[25] Y.S. Amhis, et al., HFLAV, arXiv:1909.12524 [hep-ex].